Open Access

Catalysis Research

LIDSEN Publishing Inc.

Research Article

Organic Structure-Directing Agent Free Synthesis of Mordenite with Seeds, Used as A Support for Mo Catalysts in the Transesterification of Soybean Oil

Erivaldo G. Lima [†], Fabiana N. M. Silva [†], Tellys Lins A. Barbosa [†], Meiry Gláucia Freire Rodrigues [†,*]

Federal University of Campina Grande, Academic Unit of Chemical Engineering, Av. Aprígio Veloso, 882-Bodocongó, 58109-970, Campina Grande-PB, Brazil; E-Mails: erigenuino@hotmail.com; fabymdeirosquimica@gmail.com; tellyslins@hotmail.com; meiry.freire@eq.ufcg.edu.br

† These authors contributed equally to this work.

* **Correspondence:** Meiry Gláucia Freire Rodrigues; E-Mail: meiry.freire@eq.ufcg.edu.br

Academic Editor: Narendra Kumar

Special Issue: Applied Catalysis for a Circular Economy

Catalysis Research
2023, volume 3, issue 2
doi:10.21926/cr.2302015

Received: December 20, 2022
Accepted: March 28, 2023
Published: April 07, 2023

Abstract

This work prepared mordenite using seeds and without organic structure-directing agents (OSDAs). The Mo/Mordenite was prepared through wet impregnation and the catalysts' performance was checked for transesterification of soybean oil with methanol. The mordenite zeolite was prepared through hydrothermal crystallization under static conditions with a molar composition of $6Na_2O:Al_2O_3:30SiO_2:780H_2O$. The catalyst samples were characterized crystallinity through X-ray diffraction, elemental composition by X-ray fluorescence spectroscopy, Surface areas by N_2 adsorption-desorption, surface morphology scanning electron microscopy, functional group by infrared spectroscopy and active sites by temperature programmed desorption of ammonia. The transesterification of soybean oil was carried out using the following parameters: 5% catalyst by weight, 1:12 oil to methanol molar ratio, at 200°C for either 12 h or 24 h. X-ray diffraction patterns showed the characteristic peaks of the mordenite structure. After molybdenum oxide was added, the structure of

mordenite zeolite was conserved while the specific surface area was reduced. The morphology can be described as a highly crystalline material with well-defined crystalline particles having a spherical profile characteristic of the typical morphology of sodium mordenite zeolite with a low silicon/aluminum ratio. The catalyst samples exhibited sites of a weak and medium-strength nature. The higher activity of the catalyst (Mo/Mordenite) about mordenite zeolite, could be justified by the existence of molybdenum. The wet impregnation of metal (Mo) on the surface of the MOR zeolite is an effective option to increase the acidity of the solid catalysts. Mordenite with 8.84% Mo could be a promising catalyst for the biodiesel factory.

Keywords
Mordenite zeolite synthesis; seed; organic structure-directing agent; molybdenum oxide; alternative fuel; biodiesel; transesterification; renewable energy; thermogravimetry

1. Introduction

The world is confronting an energy crisis due to the important demand for energy from fossil fuels, such as natural gas, coal and oil, which play with the raw material needs of several industries (chemical, petrochemical and pharmaceutical industries, among others). Therefore, the demand for these non-renewable sources of energy is increasing expressively. Fast consumption of fossil fuel reserves, greenhouse gas emissions and associated climate change are spurring the development of sustainable energy sources derived from renewable resources [1].

The prevalent sources of global energy supply are natural gas, coal and crude oil. However, attention is turning to fuels derived from biomass, called biofuels for energy production [2]. One such liquid biofuel is biodiesel, which has several advantages compared to conventional fossil diesel. These advantages are its non-toxicity, biodegradability, renewability, and low exhaust emissions due to the absence of sulfur and aromatics [3].

Biodiesel is a mixture of mono-alkyl esters of long-chain fatty acids derived from animal fats or vegetable oils, according to ASTM D6751 specifications for use in diesel engines. Fuel-grade biodiesel must be produced to rigorous industry standards to ensure proper performance. Biodiesel is non-toxic, biodegradable, and has a low emission profile. Chemically, biodiesel is composed of fatty acid methyl esters (FAME) that are called biodiesel only when used as fuel in diesel engines and heating systems [3, 4].

For commercial fuel use, biodiesel must be evaluated according to international standards. Some specifications have been defined, but ASTM D6751 and EN 14214 standards are the most commonly used [5, 6].

The methods for obtaining biodiesel are: direct use of vegetable oil, microemulsion, thermal cracking (pyrolysis), and transesterification [6, 7]. The direct use of vegetable oil does not apply to most diesel engines, as the high viscosity would damage the engine. The biodiesel obtained from the microemulsion and thermal cracking methods would lead to incomplete combustion due to a low cetane number. Biodiesel is most commonly produced by the transesterification method due

to its simplicity and has been widely studied and used industrially to convert vegetable oil into biodiesel [8-14].

Transesterification can be defined as the chemical process through which triglyceride molecules present in animal fat or vegetable oil react with an alcohol in the presence of a catalyst to form esters and glycerol. The first step in the transesterification is the conversion of triglycerides to diglycerides, then converting higher glycerides to lower glycerides and then to glycerol, producing one methyl ester molecule from each glyceride in each step [15-17].

The nature of the catalyst employed during transesterification is critical to the process of transforming triglycerides into biodiesel. Studies have been conducted on heterogeneous catalysts to find solutions to problems caused by the use of homogeneous catalysts in the production of biodiesel [18].

Zeolites are microporous crystalline solids with well-defined structures containing aluminum, silicon and oxygen in their cations. Mordenite zeolite is one of the high-silica zeolites and was first synthesized by Barrer in 1948, based on natural synthesis conditions [19]. The mordenite framework is composed of two channels: the main channel, parallel to [001] with a diameter of 6.6 Å, is interconnected by a smaller channel, parallel to [010] with a diameter of 2.8 Å [20-22]. Mordenite zeolite belongs to the orthorhombic crystalline system consisting of three mutually perpendicular crystallographic axes with different lengths (a = 18.1, b = 20.5 and c = 7.5 Å). This is an important feature, because the diffusion process is slow compared to other two-dimensional or three-dimensional molecular sieves (13X and 4A) [23, 24].

Adding seed crystals to a crystallization system typically increases "crystallization'' rates. This fact might be due simply to increasing the rate at which solute is integrated into the solid phase from solution due to the increased available surface area. However, it also might result from enhanced nucleation of new crystals. Understanding the specific role of seed crystals is a current area of investigation. The secondary nucleation mechanism, referred to as initial breeding, results from microcrystalline dust being washed off of seed crystal surfaces in a new synthesis batch, and has been reported in zeolite systems [25, 26].

Mordenite zeolite usually is usually carried out at temperatures ranging from 130°C to 170°C. Most mordenite syntheses use a $Na_2O/SiO_2/Al_2O_3$ system, where the hydrated Na^+ cation can be a templating agent.

Mordenite zeolite has several applications in chemical processes. However, the high cost of producing these materials with organic structure directing agents (OSDAs) is generally avoided in commercial zeolite production due to the economic and environmental disadvantages associated with preparing and removing organics occluded within zeolite micropores.

The SiO_2/Al_2O_3 ratio during synthesis is usually confined to a narrow range in the initial reactant mixture, and the reported SiO_2/Al_2O_3 ratio of mordenite products usually ranges from 8 to 18 Å. A high SiO_2/Al_2O_3 ratio for mordenite zeolite can be achieved through acid leaching of aluminum or preparation using a template. However, templates comprise a considerable portion of the total starting material cost. Additionally, in the conventional synthesis process using a template, post-synthetic calcination is required to remove the template. Treatment of wastewater and gas produced in post-processing further increases energy consumption. Considering the high costs and the energy and environmental burden caused by OSDAs, an OSDA-free synthesis is preferable. Synthetic mordenite may appear with different morphologies, such as needle-like, prismatic, flat, and parallel acicular, depending on the conditions under which it was prepared. Parameters such as

alkalinity, the SiO_2/Al_2O_3 ratio of the initial reactant mixture, seeding conditions, and the aging time have been found to signicantly influence the crystallization rate of mordenite, as well as its morphology. Using conventional methods, it can take several days to prepare mordenite zeolite. Though it has been described that microwave heating can result in a shorter synthesis period, it still requires several hours. An ultrafast synthesis of mordenite has not yet been achieved [27, 28].

Zeolites are used as a support material for the transesterification catalyst [29-32].

Results reported in Table 1 represent various catalysts prepared and characterized by different authors for biodiesel production by transesterification of vegetable oil reported in the literature [29-32].

Table 1 Summary of biodiesel conversion using several heterogeneous catalysts.

Reaction Conditions	**Al-Jammal et al., 2016** [29]	**Du et al., 2018** [30]	**Ramos et al., 2008** [31]	**Silva et al., 2019** [32]
Catalyst	1.4MKOH/TZT	NaY zeolite La_2O_3	NaX zeolite MOR Zeolite Beta Zeolite	MoO_3/Mordenite zeolite
Feedstock	sunflower oil	Castor oil	sunflower oil	soybean oil
[a]t (h)	2	-	7	2
[b]T (°C)	50	50-75	60	200
Alcohol/Oil	Methanol 1.51:1	Ethanol	Ethanol 6:1	Methanol 12:1
[c]A (rpm)	800	-	500	Without agitation
Yield (%)	98.0	85.0	-	75.4

[a]t: reaction time; [b]T: reaction temperature; [c]A: reaction agitation.

In order to compare the performance of the catalyst prepared in this literature (MoO_3/Mordenite zeolite) with recent studies, despite the experimental conditions being very different, it is possible to conclude that the catalyst prepared in this work is promising.

When comparing the conversions of the catalyst prepared in this work and the catalysts in the literature [29-31], a lower conversion value (75.4%) is evidenced, emphasizing that the system did not have agitation, the reaction temperature used was 200°C and use of methanol. Most likely using an agitated system, this temperature will be reduced and the conversion will be increased. It can also be emphasized that the Mordenite zeolite was prepared without a template, reducing the catalyst's cost.

The authors [32] has been studied the catalytic performance of mordenite and MoO_3/MOR for the transesterification of soybean oil using a batch reactor at 200°C. The effects of catalyst (Mordenite and MoO_3/MOR) on the kinematic viscosity of produced biodiesel and conversion were investigated. A preliminary design assessment shows that this catalyst (MoO_3/MOR) is sufficiently active achieving conversion over 75% at temperatures below 200°C.

The catalytic performance of Molybdenum catalysts in the reactor of transesterification reactions has been studied [33-36].

The current work used mordenite zeolite as a catalyst and catalyst support. Due to its high thermal and acidic stability and catalytic activity, mordenite zeolite has industrial importance in

catalytic processes used in petrochemical refining [37]. Characteristics such as high acidity and thermal and chemical stability are important and make this zeolite very interesting to be used as catalytic support [38, 39]. In this article, a green synthesis route to prepare mordenite was proposed. This work aimed to synthesize mordenite zeolite without organic structure-directing agents using seeds and investigate the effect of Mo on the mordenite catalyst in biodiesel production.

2. Materials and Methods

2.1 Materials

All chemicals and solvents were purchased from commercial suppliers, including Sodium hydroxide NaOH (Merck), Sodium aluminate $NaAlO_2$ (Reagen), Aerosil silica 380 SiO_2 (Evonik), ammonium molybdate $(NH_4)6Mo_7O_{24}.4H_2O$ (Synth), methanol CH_3OH (Neon), soybean oil (Soya). Deionized water was used.

2.2 Synthesis of Mordenite Zeolite

Mordenite zeolite was synthesized according to the procedure proposed by the authors [38] with some adjustments. The composition of the reaction mixture was: $6Na_2O:Al_2O_3:30SiO_2:780H_2O$. Sodium hydroxide was dissolved in deionized water, then sodium aluminate was added to the starting solution at 25°C, this mixture was added to Aerosil silica 380 and 1% of mordenite seed. As a seed for the preparation, commercial mordenite CBV-21 A was used supplied by Zeolyst International. Herein, Mordenite zeolite commercial was selected as seeds to transform and then recrystallize to target MOR zeolite, in which this conversion is favored thermodynamically and kinetically. The reaction mixture was then removed from a Teflon-lined autoclave and kept static at 170°C for 24 h. After this time, the solid was recovered by filtration, washed until reaching neutral pH (≈7) and dried at 80°C overnight.

2.3 Synthesis of Catalyst-Mo-Loaded Mordenite Prepared by AHM

The incorporation of MoO_3 into the mordenite zeolite was performed from ammonium heptamolybdate salt $[(NH_4)6Mo_7O_{24}.4H_2O]$ using impregnation [35-38]. The desired MoO_3 content in the final catalyst were 8 wt%. In a synthesis, 1.0 g of mordenite zeolite was impregnated with an aqueous solution of the molybdenum precursor [40-42]. After impregnation, the material was dried in an oven at 80°C for 4 h. Material was calcined in a muffle furnace from room temperature up to 550°C, using a 5°C/min heating ramp remaining at the final temperature (550°C) for 4 h.

2.4 Characterization

The crystal phases samples X-Ray Diffraction (XRD) of the materials were carried out on a Shimadzu XRD 6000 using Cu Kα radiation at 40 kV/30 mA, with a goniometer velocity of 2°/min and step of 0.02° in the 2θ range from 3.0° to 70.0°.

The morphology was characterized by Scanning Electron Microscopy (SEM) obtained through a scanning electron microscope TESCAN, model VEGA3.

The textural characteristics of the samples were investigated by isothermal gas adsorption/desorption of N_2 at -196°C using Micrometrics ASAP 2020 equipment.

The elemental analysis was determined through energy-dispersive X-ray spectrophotometry, in a Shimadzu EDX-700 instrument.

The infrared spectroscopy was realized using a Nicolet Avatar infrared spectrophotometer AVATAR TM 360 FT-IR E.S.P. (Thermo Electron Corporation, USA), in the wavelengths in the range from 4000 to 400 cm^{-1}.

Temperature-programmed desorption of ammonia (NH_3-TPD) was conducted on a quartz reactor and heated at a rate of 10°C/min until reaching 500°C under helium flow (30 mL/min), remaining at this temperature for 1 h. The pretreatment was aimed at removing the physio-acid sites of the catalyst. The system was then cooled to 100°C and Subjected to an ammonia flow for 40 minutes. After that, the sample was with helium over 1 h at 100°C to remove NH_3 molecules physicians. The system was then heated at a rate of 10°C/min to 800°C under helium flow, monitoring the amount of ammonia desorbed as a function of the a thermal conductivity detector (TCD).

2.5 Characterization of Soybean Oil and Biodiesel

The quality measurements of biodiesel and the physical and chemical properties of oil were valued.

2.5.1 Kinematic Viscosity

Measurements were performed based on ASTM D445 (ASTM D445-17, Standard Test Method for Kinematic Viscosity of Transparent and Opaque Liquids (and Calculation of Dynamic Viscosity), ASTM International, West Conshohocken, PA; 2017) [43] with a Cannon Fenske viscometer. The kinematic viscosity of samples was valued at 40°C.

Kinematic viscosity was obtained using Equation 1:

$$\mu = kt \tag{1}$$

where k is 0.2407 mm^2/s^2 is the constant inherent to the viscometer used and t (s) is the liquid flow time through the capillary.

2.5.2 Specific Mass

The specific mass of the samples was measured at 20°C with a digital densimeter Anton Paar densitometer, model 30px. A 2-mL aliquot of biodiesel was added to the densimeter and the result was recorded, based on ASTM D 4052 [ASTM] [44].

2.5.3 Free Acid Content

The determination of free acids content in the sample solution was carried out by titration with NaOH, based on IUPAC standards [45]. The solution acidity was determined according to Equation 2:

$$\text{Free Acid Content} = \frac{(V - PB).F.M.\left(40\frac{g}{mol}\right)}{P} \tag{2}$$

V is the volume of NaOH used by the sample (mL), P is sample mass in grams, F is the correction fator, PB is the volume spent on the blank and M is NaOH mol/L.

2.6 Thermal Study of Biodiesel

Thermogravimetric (TG) curves were carried out using a thermobalance (SHIMADZU – DTG – 60 models) in the temperature range of 50-600°C, under a nitrogen atmosphere flowing at a rate of 100 mL/min, using an alumina crucible of 70 µL and heating rate 10°C/min.

2.7 Catalytic Activity

The reaction transesterification of soybean oil determined the catalytic activity with methanol was performed in a system comprised of a batch reactor (autoclave stainless steel). The reaction conditions were: temperature of 200°C with 12 and 24 h of reaction, using a molar ratio of 1:12 (soybean oil/methanol) and 5% of catalyst related to the mass of soybean oil utilized. Then, the mixture was transferred to a separation funnel for phase separation. Two phases were observed: the methyl ester and the glycerin. The biodiesel samples were submitted to a washing process to purify the esters with distilled water, then centrifuged at 600 RPM for 30 minutes and dried at 100°C [40-42, 46-48].

The system for transesterifying soybean oil with methanol to produce biodiesel in a batch reactor without agitation can be seen in Figure 1.

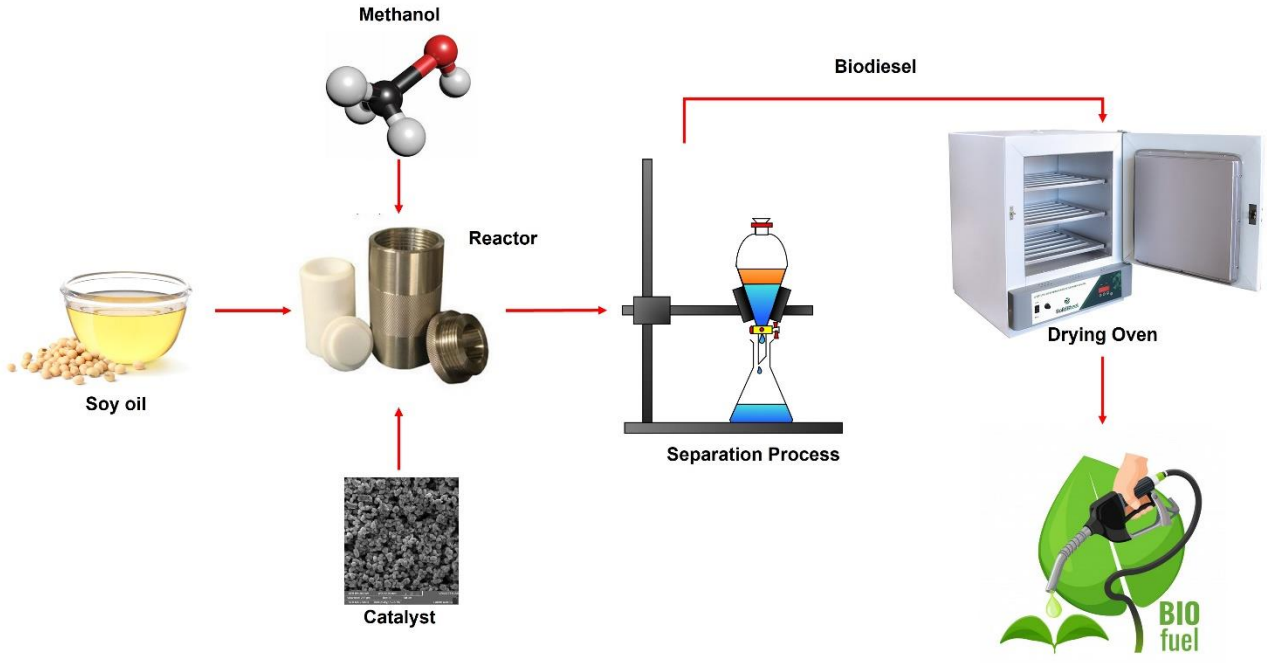

Figure 1 System for transesterification of soybean oil with methanol to produce biodiesel in a batch reactor.

3. Results and Discussion

3.1 Characterization

Figure 2 (A) shows the XRD patterns of the mordenite zeolite samples exhibit the characteristic diffraction peaks of the mordenite structure and evidence the phase purity of the samples, exhibiting sharp reflection peaks from 5° to 70° that are characteristic of zeolite and that demonstrate the presence of highly crystalline mordenite.

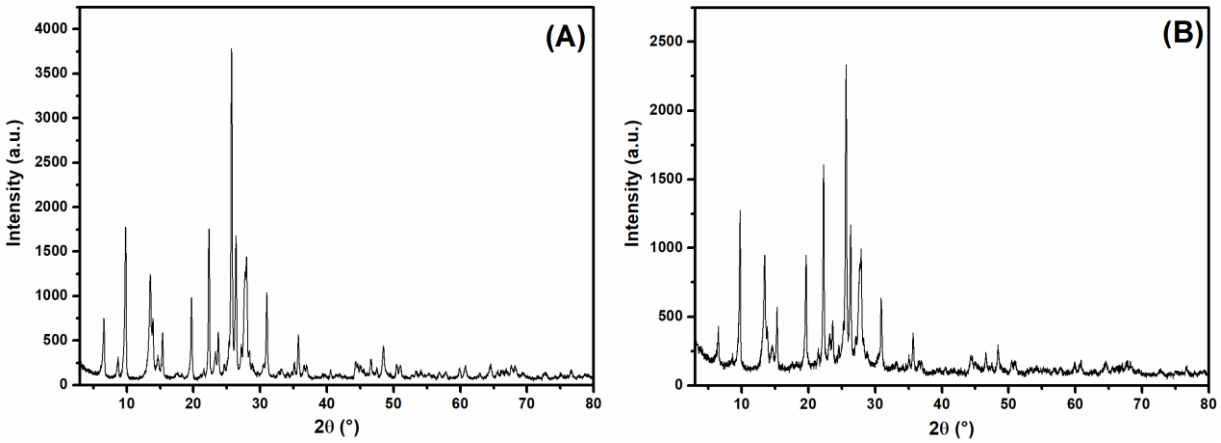

Figure 2 X-ray powder diffraction patterns of the (A) Mordenite zeolite and (B) MoO_3/Mordenite samples after the impregnation and calcination process.

Figure 2 (B) presents the X-ray powder diffraction patterns of Mo-impregnated Mordenite zeolite. The notable crystalline lines in the diffraction pattern of Mordenite zeolite are identical to those recorded in the X-ray data file (JCPDS, No. 80-0645) for phase identification. Catalysts showed XRD patterns that fit the structure of mordenite, with indexed peaks at 2θ = 9.8, 19.59, 22.4, 25.8, 26.4, 27.7, and 30.9°, as presented in Figure 2 (A) and 2 (B). The structural stability of Mordenite remains preserved during the initial stage of molybdenum addition. The structural integrity was indicated by comparing these spikes with those found for mordenite in its sodium form [33, 38, 44]. No crystalline feature characteristic of a separate MoO_3 phase in the MoO_3/Mordenite patterns was detected. These data imply a homogeneous distribution of oxo molybdenum species as small oligomers within the pores or on a nearby zeolite surface during molybdenum addition. The oxo molybdenum species will tend to become uniform throughout the internal zeolite surfaces.

Detailed analysis of the X-ray diffraction patterns of the samples did not show evidence of a MoO_3 phase.

Figure 3 presents the N_2 adsorption/desorption isotherms at -196°C for Mordenite zeolite and the MoO_3/Mordenite catalyst.

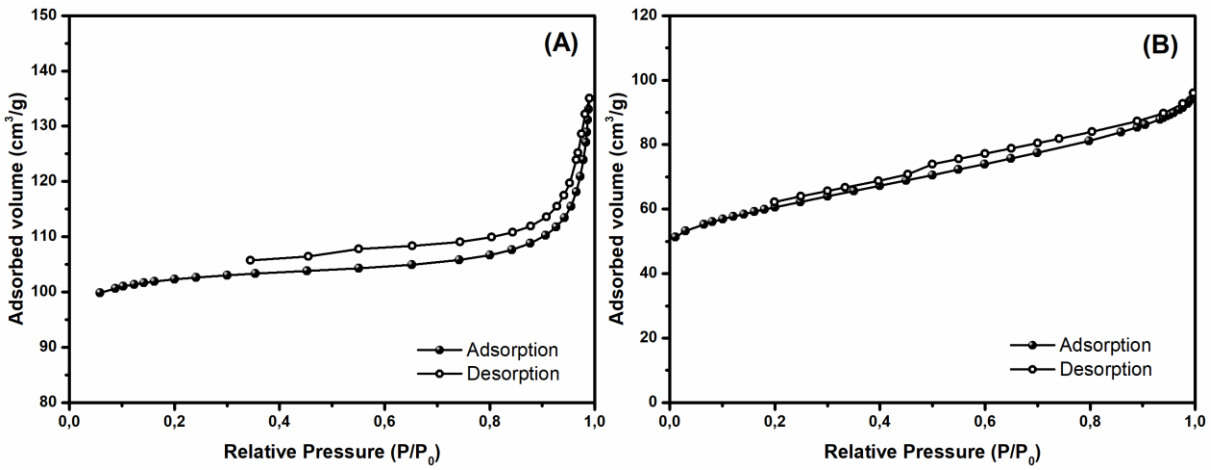

Figure 3 N_2 adsorption (filled square)-desorption (open square) isotherms of the calcined molecular sieves (A) Mordenite and (B) MoO_3/Mordenite catalyst.

A similar isotherm profile is observed for the catalysts, classified by IUPAC as type I, characteristic of microporous materials. This isomorphism predominates in materials where adsorption occurs at very low relative pressures with a high volume of adsorbed N_2, due to the strong interaction between pore walls and adsorbate, occurring at relative pressures of up to 0.3 of the adsorption of the monolayer. Higher pressure is required to fill pores and form multiple layers, which may favor interaction between the adsorbed molecules. For relative pressure greater than 0.3, multilayers and capillary condensation formation is obtained through maximizing adsorption. Once the micropores are filled, adsorption continues on the outer surface, but in this type of isotherm, the outer surface is relatively small. This is considered reversible as the adsorption and desorption processes have very close or coincident isotherms. Hysteresis is classified as H4, predominantly found in solids consisting of aggregates or particle agglomerates forming uniform slit-like pores and sharp particles such as cubes or plates [49-53].

The results showed in Table 1 for the textural analysis presented that the mordenite zeolite had a specific surface area of 343 m^2/g (calculated using the BET method) agreeing with the literature [38, 52-53], where values from 50 to 450 m^2/g are found for mordenite zeolite synthesized under stable hydrothermal conditions with or without an organic structure-directing agent. The volume of micropores, 0.144 cm^3/g, calculated by NLDFT is by the literature, ranging from 0.130 to 0.280 cm^3/g, values characteristic of sodium mordenite zeolite.

The microstructure and characteristics of the mordenite zeolite and modified zeolite (MoO_3/Mordenite), that is specific surface area and pore size, were measured by nitrogen physisorption and successive mathematical treatments of the adsorption data (Table 2).

Table 2 Summary of textural parameters determined for Mordenite and MoO_3/Mordenite catalyst.

	S_{BET} (m^2/g)[a]	V_P (cm^3/g)[b]	Dp BJH (nm)	a	b	c	Cell volume
Mordenite	343	0.2044	15.1	18.08	17.67	7.28	2325.77
MoO_3/Mordenite	207	0.0774	4.8	18.16	20.49	7.52	2798.36

[a]S_{BET}: Specific surface area obtained by BET method; [b]V_P: total volume pores.

The results of the elemental analyses obtained for catalysts are presented in Table 3. According to the data, it is possible to verify that the Mordenite zeolite showed a high percentage of silicon oxide (SiO_2). Sodium is considered to be a structural compensation cation (Table 3) [54]. After impregnation, the XRF analyses performed revealed that 8.8% MoO_3 was effectively incorporated into the mordenite (MOR) structure.

Table 3 Chemical analysis of the samples.

Samples	SiO_2 (%)	Al_2O_3 (%)	Na_2O (%)	MoO_3 (%)	Others (%)	Si/Al molar ratio
Mordenite	76.4	14.9	7.6	-	0.9	9.1
MoO_3/Mordenite	68.2	12.0	5.8	8.8	5.1	-

Figure 4 presents the SEM images of the Mordenite and MoO_3/Mordenite catalyst.

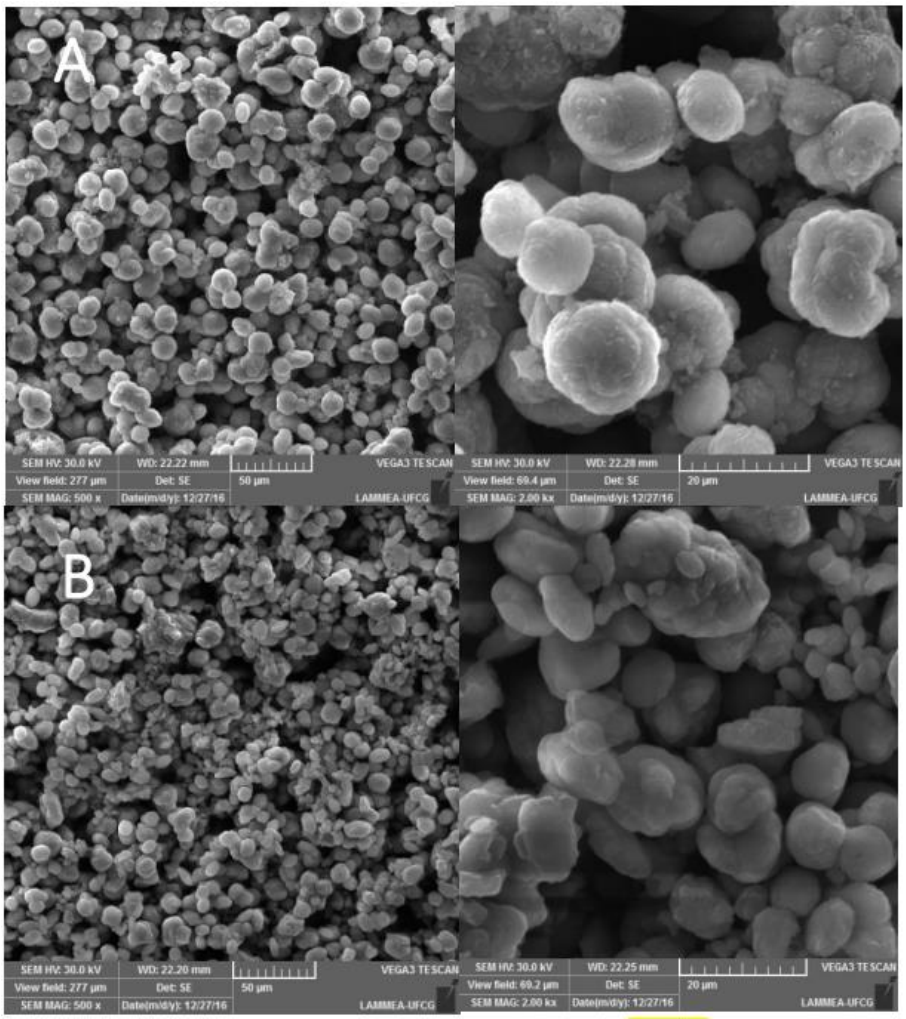

Figure 4 SEM micrographs of the (A) Mordenite and (B) MoO_3/Mordenite samples.

The typical characteristics of the mordenite zeolite prepared with the addition of seeds are a high degree of crystallinity with the presence of defined crystalline particles having a spherical profile, characteristic of the typical morphology of sodium mordenite zeolite with low synthesis (Figure 4

(A)) [27]. Based on ImageJ studies, the particle size was analyzed and measured from SEM imagery using the ImageJ software (National Institute of Health). The average particle size of zeolite was found to be 10.60 µm. According to SEM imagery (Figure 4 (B)), the sample consisted of irregularly-shaped particles with an average size of 75.74 µm. MoO_3 impregnation seems to change the morphology of mordenite.

The presence of metal oxide alloy seems to increase the heterogeneity of the catalyst particle size and the particle size itself.

The FTIR spectra of Mordenite zeolite and MoO_3/Mordenite catalyst are presented in Figure 5. The infrared spectrum framework of Mordenite (Figure 5 (A)) is in agreement with previously-found data [55].

The absorption bands at 713, 793, 1030, and 1222 cm^{-1} are due to the T-O bending, internal and external symmetric stretching (←OT→), internal and external asymmetric stretching (←OT→←O) vibrations corresponding to siliceous materials. The broadband in the 3440 cm^{-1} is due to the stretching vibration of the isolated silanol groups (Si-O-H) and the stretching of the water molecules absorbed on the solid surface [56].

Thus, both XRD and FTIR experimental results reveal that the mordenite structure is retained, even after the impregnation of MoO_3.

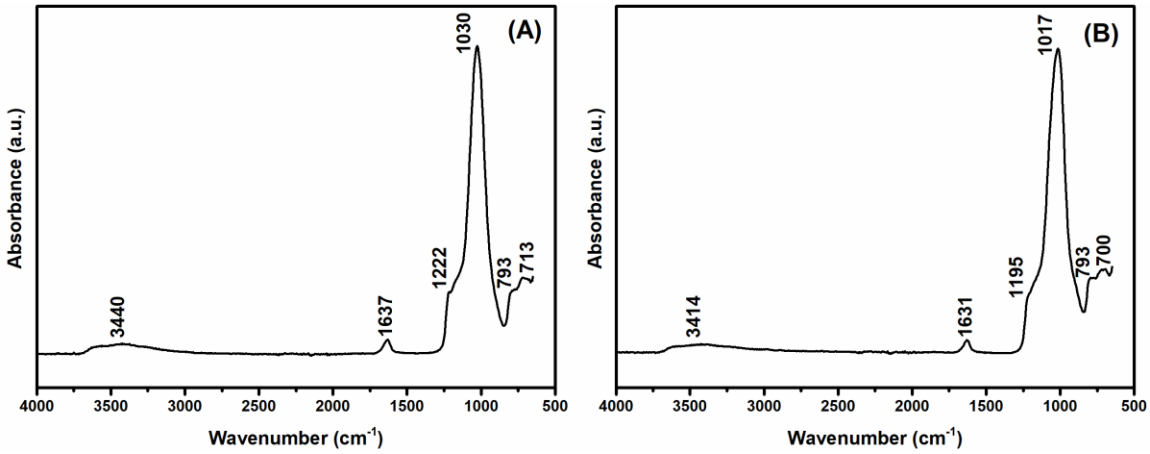

Figure 5 FTIR spectra of (A) Mordenite and (B) MoO_3/Mordenite catalyst.

The acidity of the prepared samples was evaluated using thermos-programmed ammonia desorption (NH_3-TPD), which makes it possible to obtain the total number of acid sites and the relative distribution of forces [57].

The NH_3-TPD profile of mordenite zeolite and MoO_3/Mordenite are shown in Figure 6.

It is seen that the profile is essentially made up of an NH_3 desorption peak in the range of 150°C-400°C (Figure 6(A) e 6(B)). High concentrations of weak and medium-strength sites are present, where the intensity of the peak is directly proportional to the concentration of the acid sites present in the catalyst [58-60]. The peak at lower temperatures has been proven due to weakly held ammonia, probably hydrogen bonded, but not the ammonia species adsorbed on the acid site. In the MoO_3/Mordenite catalyst, the acidity provided by the presence of molybdenum in the oxide form observed in the desorption curves of NH_3 can be indicated by the presence of weak sites occurring in the 150°C-350°C temperature range for all catalysts, which are generated by the presence of MoO_3 and other species.

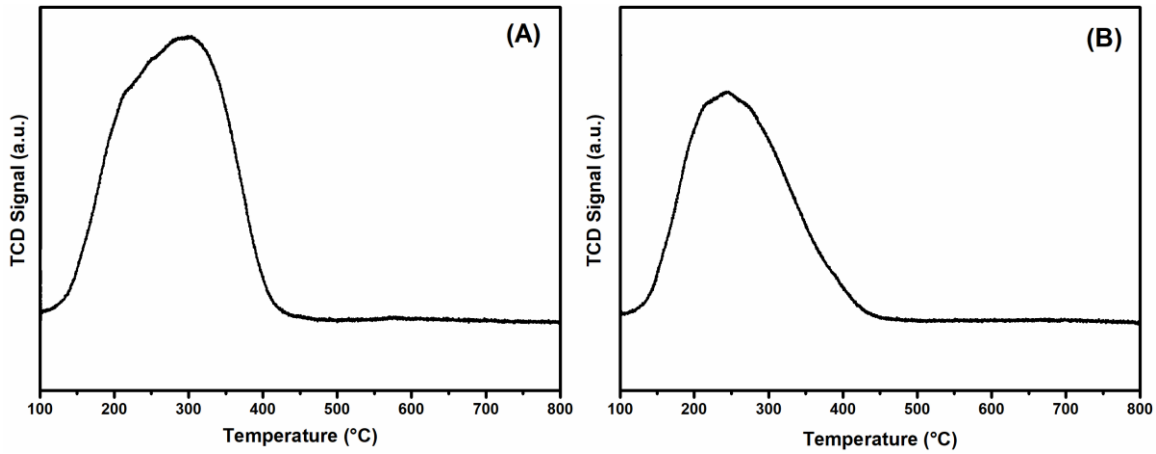

Figure 6 NH_3-TPD Profiles of samples (A) Mordenite and (B) MoO_3/Mordenite catalyst.

3.2 Synthesis of Biodiesel

The specific mass and kinematic viscosity are physicochemical parameters of great relevance that are indicative of the conversion of triglycerides to esters, caused by the reduction that occurs during the cracking of the major triglyceride, diglyceride, and monoglyceride chains into methyl esters having smaller chains [30].

The results for specific mass, kinematic viscosity, reduction of soybean oil viscosity, and all reaction products obtained from the reaction and conversion of ester are presented in Table 4. ASTM D6751 standards specify the limits for the density of the diesel and biodiesel samples.

Table 4 Physicochemical characterization of the biodiesel produced from soybean oil.

Samples	**t (h)**	**12**	**24**	**Limits ASTM D6751**	**Limits ANP 45/2014**
Soybean oil	Viscosity (mm^2/s)	34.30			
	Specific mass (g/cm^3)	0.922			
Mordenite	Viscosity (mm^2/s)	10.3	7.3	1.9-6.0	3.0-6.0
	Reduction (%)	70.0	78.7		
	Specific mass (g/cm^3)	0.903	0.897		0.85-0.90
	Acid values (mg KOH)	0.53	0.56		<0.5
MoO_3/Mordenite	Viscosity (mm^2/s)	7.7	6.4		
	Reduction (%)	77.5	81.3		
	Specific mass (g/cm^3)	0.900	0.893		
	Acid values (mg KOH)	0.54	0.43		

According to Table 4, kinematic viscosity decreases with the reaction, with reductions of 70.0% and 77.5% for the reaction time of 12 h and 78.7 and 81.3 for the reaction time of 24 h.

The specific mass values were observed to decrease, when compared with the value for soybean oil. It is possible to see a positive effect from the presence of Mo, where kinematic viscosity decreased rapidly during the first hours of the reaction. These reductions are caused by a decrease in unsaturation from the breakdown of triglyceride chains, benefiting the formation of smaller molecules with lower amounts of unsaturation.

For the reaction times shown in Table 4, the kinematic viscosity and specific mass results were unsatisfactory compared to the specifications found in ANP 45/2014 and ASTM D6751.

3.3 Thermal Stability

The stability of these catalysts is a very relevant issue [61-63].

Thermogravimetric analyses (TG/DTG) were carried out to measure the transesterification reaction through the difference in volatilization temperature of triglycerides and esters [64]. Through this, it was possible to determine the yield from the transesterification reaction and the total ester content.

Thermogravimetric analysis of biodiesel is not a standard method for biodiesel characterization. However, the authors [65] shows that TGA is a fast and simple method for accurately monitoring the triglyceride conversion stages and the purity of the final product during biodiesel production, without the need for extensive sample preparations and expensive standard solutions.

The TG/DTG analysis made it possible to determine the thermal behavior of the soybean oil and methyl biodiesel samples, as shown in Figure 7.

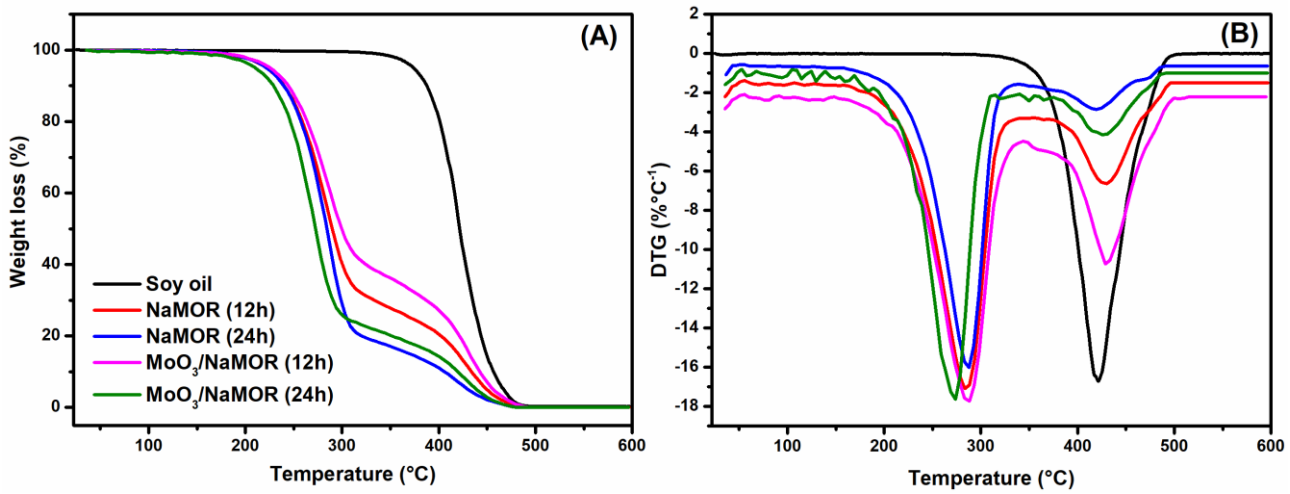

Figure 7 TG/DTG curves for soybean oil in N_2 products obtained from the reaction at 12 h and 24 h with catalysts.

The mass of the soybean oil decreases at approximately 350°C, and it continues its decrease until all the soybean oil present in the sample is vaporized.

All of the curves show two mass losses due to the volatilization of methyl esters at about 200°C-350°C and unconverted triglycerides at about 350°C-500°C. The TG curves for the products of the reactions with Mordenite and MoO_3/Mordenite catalysts presented two mass losses assigned to the volatilization of methyl ester and decomposition of unconverted triglycerides, according to the biodiesel DTG curves (Figure 7). The biodiesel samples' TG curve profiles displayed different behavior regarding peak intensity, which is directly proportional to the mass loss and related to the reaction time, amount of esters and/or triglycerides, and catalyst activity in the transesterification reaction [64].

The values for the temperature ranges and percentage of mass loss for each step are shown in Table 5.

Table 5 Representative TG data of the samples in N_2 atmosphere.

Sample	Time (h)	Steps	Temperature range (°C)	Event mass loss (%)
Soybean oil		1st		
Mordenite	12	1st	173.6 – 324.6	67.7
		2nd	324.6 – 485.8	31.1
	24	1st	183.2 – 325.8	79.2
		2nd	324.8 – 475.3	19.2
MoO_3/Mordenite	12	1st	178.5 – 328.1	59.7
		2nd	328.1 – 488.9	39.0
	24	1st	154.2 – 313.2	80.6
		2nd	313.2 – 476.0	19.3

Table 5 shows the mass losses related to the volatilization of methyl esters (biodiesel) and unconverted triglycerides, for reactions with the MoO_3/Mordenite catalyst. The greater intensity of the peaks (150°C-350°C) observed in the DTG graphs indicates a greater amount of methyl esters, with a higher degree of conversion of triglycerides to methyl esters. The other catalysts showed results below 70% for the number of methyl esters and a greater presence of unconverted triglycerides [31].

The authors [63] analyzed the biodiesel produced from sunflower oil in the presence of ethyl alcohol through thermogravimetry (TG) in a system adapted with reflux, where the biodiesel obtained in the transesterification reaction presented different profiles according to the catalyst used in the reaction. However, the thermogravimetric analysis indicated the presence of two regions of mass loss for all curves, attributed to the volatilization of ethyl esters (160°C-320°C) and the volatilization of unconverted triglycerides (320°C-440°C).

The authors [64] studied thermogravimetric curves for biodiesel produced with methanol in a PARR reactor. They observed the greatest mass loss at about 135°C to 344°C with a total mass loss of 98.6%, attributed to the combustion or volatilization of the methyl esters formed as products of the transesterification reaction of sunflower and cotton oils. Another mass loss occurred in the temperature range from 304°C to 409°C, attributed to volatilization and/or combustion of unconverted triglycerides.

4. Conclusions

In this study, preparing mordenite zeolite without organic structure-directing agents (OSDAs) using seeds was possible in 24 h at 170°C. The formation of mordenite zeolite was proven through characterization techniques.

According to the XRF results, the molybdenum incorporated into the mordenite zeolite supports was close to theoretical values, evidencing the effectiveness of wet impregnation. After incorporation with molybdenum oxide, the mordenite zeolite structure was preserved. As evidenced by X-ray diffraction results, Mo species exist as highly dispersed surface species.

Biodiesel was produced using two heterogeneous catalysts (Mordenite and Mo/Mordenite). The greater activity of the Mo/Mordenite catalyst, concerning the mordenite zeolite, can be explained by the presence of molybdenum.

It can be concluded that, under the conditions studied (batch reaction without stirring, temperature of 200°C, 5% catalyst, 1:12 soybean oil/methanol ratio, and addition of molybdenum) the production of biodiesel was positively affected.

Acknowledgments

The authors would like to make special acknowledgements to the Coordenação de Aperfeiçoamento de Pessoal de Nível Superior (CAPES) for their financial support to this research.

Author Contributions

Erivaldo G. Lima: Investigation, Formal analysis; Fabiana N. M. Silva: Investigation, Formal analysis; Tellys L. A. Barbosa: Investigation, Formal analysis, Writing – Original Draft; Meiry G. F. Rodrigues: Conceptualization, Formal analysis, Funding acquisition, Writing – Review & Editing.

Funding

Coordenação de Aperfeiçoamento de Pessoal de Nível Superior (CAPES).

Competing Interests

The authors have declared that no competing interests exist.

References

1. Jeon H, Kim DJ, Kim SJ, Kim JH. Synthesis of mesoporous MgO catalyst templated by a PDMS–PEO comb-like copolymer for biodiesel production. Fuel Process Technol. 2013; 116: 325-331.
2. Kapilan N, Babu TA, Reddy RP. Technical aspects of biodiesel and its oxidation stability. Int J Chemtech Res. 2009; 1: 278-282.
3. Vicente G, Martinez M, Aracil J. Integrated biodiesel production: A comparison of different homogeneous catalysts systems. Bioresour Technol. 2004; 92: 297-305.
4. Meher LC, Sagar DV, Naik SN. Technical aspects of biodiesel production by transesterification-a review. Renew Sust Energ Rev. 2006; 10: 248-268.
5. Leung DYC, Wu X, Leung MKH. A review on biodiesel production using catalyzed transesterification. Appl Energy. 2010; 87: 1083-1095.
6. Borges ME, Díaz L. Recent developments on heterogeneous catalysts for biodiesel production by oil esterification and transesterification reactions: A review. Renew Sust Energ Rev. 2012; 16: 2839-2849.
7. Helwani Z, Othman MR, Aziz N, Fernando WJN, Kim J. Technologies for production of biodiesel focusing on green catalytic techniques: A review. Fuel Process Technol. 2009; 90: 1502-1514.
8. Juan JC, Kartika DA, Wu TY, Hin TYY. Biodiesel production from jatropha oil by catalytic and non-catalytic approaches: An overview. Bioresour Technol. 2011; 102: 452-460.
9. Chouhan APS, Sarma AK. Modern heterogeneous catalysts for biodiesel production: A comprehensive review. Renew Sust Energ Rev. 2011; 15: 4378-4399.
10. Ma F, Hanna MA. Biodiesel production: A review. Bioresour Technol. 1999; 70: 1-15.

11. Bateni H, Saraeian A, Chad A. A comprehensive review on biodiesel purification and upgrading. Biofuel Res J. 2017; 15: 668-690.
12. Xie W, Zhao L. Production of biodiesel by transesterification of soybean oil using calcium supported tin oxides as heterogeneous catalysts. Energy Convers Manag. 2013; 76: 55-62.
13. Sankaranarayanan TM, Pandurangan A, Banu M, Sivasanker S. Transesterification of sunflower oil over MoO_3 supported on alumina. Appl Catal A. 2011; 409-410: 239-247.
14. Ramachandran K, Suganya T, Gandhi NN, Renganathan S. Recent developments for biodiesel production by ultrasonic assist transesterification using different heterogeneous catalyst: A review. Renew Sust Energ Rev. 2013; 22: 410-418.
15. Banerjee A, Chakraborty R. Parametric sensitivity in transesterification of waste cooking oil for biodiesel production—A review. Resour Conserv Recycl. 2009; 53: 490-497.
16. Vyas AP, Verma JL, Subrahmanyam N. A review on FAME production processes. Fuel. 2010; 89: 1-9.
17. Hernández-Hipólito P, Juárez-Flores N, Martínez-Klimova E, Gómes-Cortés A, Bokhimi X, Escobar-Alarcón L, et al. Novel heterogeneous basic catalysts for biodiesel production: Sodium titanate nanotubes doped with potassium. Catal Today. 2015; 250: 187-196.
18. Atadashi IM, Aroua MK, Abdul Aziz AR, Sulaiman NMN. The effects of catalysts in biodiesel production: A review. J Ind Eng Chem. 2013; 19: 14-26.
19. Barrer RM. Syntheses and reactions of mordenite. J Chem Soc. 1948; 2158-2163. doi: 10.1039/JR9480002158.
20. Lu B, Oumi Y, Sano T. Convenient synthesis of large mordenite crystals. J Cryst Growth. 2006; 291: 521-526.
21. Ma Z, Xie J, Zhang J, Zhang W, Zhou Y, Wang J. Mordenite zeolite with ultrahigh SiO_2/Al_2O_3 ratio directly synthesized from ionic liquid-assisted dry-gel-conversion. Microporous Mesoporous Mater. 2016; 224: 17-25.
22. Zhang J, Singh R, Webley PA. Alkali and alkaline-earth cation exchanged chabazite zeolites for adsorption based CO_2 capture. Microporous Mesoporous Mater. 2008; 111: 478-487.
23. Fischer F, Lutz W, Buhl JC, Laevemann E. Insights into the hydrothermal stability of zeolite 13X. Microporous Mesoporous Mater. 2018; 262: 258-268.
24. Panda D, Kumar EA. Surface modification of zeolite 4A molecular sieve by planetary ball milling. Mater Today. 2017; 4: 395-404.
25. Thompson RW. Nucleation, growth, and seeding in zeolite synthesis. In: Verified syntheses of zeolitic materials. Amsterdam, Netherlands: Elsevier Science; 2001. pp. 21-23.
26. Jain R, Rimer JD. Seed-assisted zeolite synthesis: The impact of seeding conditions and interzeolite transformations on crystal structure and morphology. Microporous Mesoporous Mater. 2020; 300: 110174.
27. Zhu J, Liu Z, Endo A, Yanaba Y, Yoshikawa T, Wakihara T, et al. Ultrafast, OSDA-free synthesis of mordenite zeolite. CrystEngComm. 2017; 19: 632-640.
28. Oleksiak MD, Rimer JD. Synthesis of zeolites in the absence of organic structure-directing agents: Factors governing crystal selection and polymorphism. Rev Chem Eng. 2014; 30: 1-49.
29. Al-Jammal N, Al-Hamamre Z, Alnaief M. Manufacturing of zeolite based catalyst from zeolite tuft for biodiesel production from waste sunflower oil. Renew Energ. 2016; 93: 449-459.
30. Du L, Ding S, Li Z, Lv E, Lu J, Ding J. Transesterification of castor oil to biodiesel using NaY zeolite-supported La_2O_3 catalysts. Energy Convers Manag. 2018; 173: 728-734.

31. Ramos MJ, Casas A, Rodríguez L, Romero R, Pérez Á. Transesterification of sunflower oil over zeolites using different metal loading: A case of leaching and agglomeration studies. Appl Catal A. 2008; 346: 79-85.
32. do Nascimento Silva FM, Lima EG, de Almeida Barbosa TL, Rodrigues MG. Evaluation of catalysts mordenite and MoO_3/mordenite in the production of biodiesel. Mater Sci Forum. 2019; 958: 11-16.
33. Mouat AR, Lohr TL, Wegener EC, Miller JT, Delferro M, Stair PC, et al. Reactivity of a carbon-supported single-site molybdenum dioxo catalyst for biodiesel synthesis. ACS Catal. 2016; 6: 6762-6769.
34. Pinto BF, Garcia MAS, Costa JCS, de Moura CVR, de Abreu WC, de Moura EM. Effect of calcination temperature on the application of molybdenum trioxide acid catalyst: Screening of substrates for biodiesel production. Fuel. 2019; 239: 290-296.
35. Chen C, Cai L, Zhang L, Fu W, Hong Y, Gao X, et al. Transesterification of rice bran oil to biodiesel using mesoporous NaBeta zeolite-supported molybdenum catalyst: Experimental and kinetic studies. Chem Eng J. 2020; 382: 122839.
36. Zhang W, Wang C, Luo B, He P, Li L, Wu G. Biodiesel production by transesterification of waste cooking oil in the presence of graphitic carbon nitride supported molybdenum catalyst. Fuel. 2023; 332: 126309.
37. Supamathanon N, Wittayakun J, Prayoonpokarach S. Properties of Jatropha seed oil from northeastern Thailand and its transesterification catalyzed by potassium supported on NaY zeolite. J Ind Eng Chem. 2011; 17: 182-185.
38. Kim GJ, Ahn WS. Direct synthesis and characterization of high-SiO_2-content mordenites. Zeolites. 1991; 11: 745-750.
39. Sano T, Wakabayashi S, Oumi Y, Uozumi T. Synthesis of large mordenite crystals in the presence of aliphatic alcohol. Microporous Mesoporous Mater. 2001; 46: 67-74.
40. Rodrigues JJ, Marinho JC, Eduardo RS, Lima EG, Rodrigues MGF. Study of the application of Mo/SBA-15 and Ni/SBA-15 catalysts, prepared by microwave heating, in the synthesis of biodiesel. Braz J Pet Gas. 2015; 9. doi: 10.5419/bjpg2015-0002.
41. Lima EG, Barbosa TLA, Vasconcelos PMN, Rodrigues MGF. Comparation of catalysts (VD and MoO_3/VD) in the transesterification of soybean oil for biodiesel production. J Eng Exact Sci. 2019; 5: 0158-0167.
42. Silva FMN, Lima EG, Rodrigues MGF. Preparation and characterization of MOR catalysts, Mo-MOR Ni-MOR and for application in the transesterification of soybean oil. 12th European congress on catalysis; 2015; Kazan.
43. American Society for Testing and Materials. ASTM D445: Standard test method for kinematic viscosity of transparent and opaque liquids (and calculation of dynamic viscosity) – eLearning Course. West Conshohocken, PA: ASTM; 2004.
44. American Society for Testing and Materials. ASTM D4052 - density, relative density, and API gravity of liquids by digital density meter. West Conshohocken, PA: ASTM; 1996.
45. IUPAC. Standard methods for the analysis of oils, fats and derivatives. Oxford, England: Blackwell; 1992.
46. Khalil U, Muraza O. Microwave-assisted hydrothermal synthesis of mordenite zeolite: Optimization of synthesis parameters. Microporous Mesoporous Mater. 2016; 232: 211-217.

47. Cid R, Llambias FJG, Fierro JLG, Agudo AL, Villasenor J. Physicochemical characterization of MoO_3-NaY zeolite catalysts. J Catal. 1984; 89: 478-488.
48. Salama TM, Othman I, Sirag M, El-Shobaky GA. Comparative study of molybdenum oxide in NaY zeolite prepared by conventional impregnation and vapor-phase deposition techniques. Microporous Mesoporous Mater. 2006; 95: 312-320.
49. Leofanti G, Padovan M, Tozzola G, Venturelli B. Surface area and pore texture of catalysts. Catal Today. 1998; 41: 207-219.
50. Kaneko K. Determination of pore size and pore size distribution: Adsorbents and catalysts. J Membr Sci. 1994; 96: 59-89.
51. Gregg SJ, Sing KSW. Adsorption, surface area and porosity. London: Academic Press; 1982.
52. Klunk MA, Schröpfer SB, Dasgupta S, Das M, Caetano NR, Impiombato AN, et al. Synthesis and characterization of mordenite zeolite from metakaolin and rice husk ash as a source of aluminium and silicon. Chem Pap. 2020; 74: 2481-2489.
53. Wojciechowska KM, Król M, Bajda T, Mozgawa W. Sorption of heavy metal cations on mesoporous ZSM-5 and mordenite zeolites. Materials. 2019; 12: 3271.
54. Guisnet M, Ribeiro FR. Zeólitos Um Nanomundo ao Serviço da Catálise. Fundação Calouste Gulbenkian; 2004.
55. Saxena SK, Viswanadham N. Enhanced catalytic properties of mesoporous mordenite for benzylation of benzene with benzyl alcohol. Appl Surf Sci. 2017; 392: 384-390.
56. Narayanan S, Vijaya JJ, Sivasanker S, Alam M, Tamizhdurai P, Kennedy LJ. Characterization and catalytic reactivity of mordenite–investigation of selective oxidation of benzyl alcohol. Polyhedron. 2015; 89: 289-296.
57. Lónyi F, Valyon J. On the interpretation of the NH_3-TPD patterns of H-ZSM-5 and H-mordenite. Microporous Mesoporous Mater. 2001; 47: 293-301.
58. Hidalgo CV, Itoh H, Hattori T, Niwa M, Murakami Y. Measurement of the acidity of various zeolites by temperature-programmed desorption of ammonia. J Catal. 1984; 85: 362-369.
59. Katada N, Igi H, Kim JH, Niwa M. Determination of the acidic properties of zeolite by theoretical analysis of temperature-programmed desorption of ammonia based on adsorption equilibrium. J Phys Chem B. 1997; 101: 5969-5977.
60. Moradi GR, Yaripour F, Vale-Sheyda P. Catalytic dehydration of methanol to dimethyl ether over mordenite catalysts. Fuel Process Technol. 2010; 91: 461-468.
61. Marchetti JM. A summary of the available technologies for biodiesel production based on a comparison of different feedstock's properties. Process Saf Environ Prot. 2012; 90: 157-163.
62. da Costa Evangelista JP, Gondim AD, Di Souza L, Araujo AS. Alumina-supported potassium compounds as heterogeneous catalysts for biodiesel production: A review. Renew Sust Energ Rev. 2016; 59: 887-894.
63. da Silva JC, Gondim AD, Galvão LP, da Costa Evangelista JP, Araujo AS, Fernandes VJ. Thermal stability evaluation of biodiesel derived from sunflower oil obtained through heterogeneous catalysis (KNO_3/Al_2O_3) by thermogravimetry. J Therm Anal Calorim. 2015; 119: 715-720.
64. Galvão LPF, Santos AGD, Gondim AD, Barbosa MN, Araujo AS, Di Souza L, et al. Comparative study of oxidative stability of sunflower and cotton biodiesel through P-DSC. J Therm Anal Calorim. 2011; 106: 625-629.

65. Alves CT, Peters MA, Onwudili JA. Application of thermogravimetric analysis method for the characterisation of products from triglycerides during biodiesel production. J Anal Appl Pyrolysis. 2022; 168: 105766.